ACS OMEGA

http://pubs.acs.org/journal/acsodf

Article

Anti-quorum Sensing and Anti-biofilm Activity of Zinc Oxide Nanospikes

Mohd. Farhan Khan,[△] Fohad Mabood Husain,[*,△] Qamar Zia,[*,△] Ejaz Ahmad, Azfar Jamal, Mohammed Alaidarous, Saeed Banawas, Md. Manzar Alam, Bader A. Alshehri, Mohd. Jameel, Pravej Alam, Mohd Imran Ahamed, Akhter H. Ansari, and Iqbal Ahmad

Cite This: *ACS Omega* 2020, 5, 32203−32215

Read Online

ACCESS | Metrics & More | Article Recommendations

ABSTRACT: This study evaluates the impact of two separate incubation periods (4 and 6 weeks) on the morphology of sol−gel-fabricated ZnO nanospikes (ZNs), that is, ZN1 and ZN2, respectively. We further analyzed the inhibitory effects of ZN1 and ZN2 on quorum sensing (QS) and biofilm formation in *Pseudomonas aeruginosa* (PAO1) and *Chromobacterium violaceum* (strains 12472 and CVO26). The size of the synthesized ZNs was in the range of 40−130 nm, and finer nanoparticles were synthesized after an incubation period of 6 weeks. Treatment with ZNs decreased the production of violacein in the pathogen without affecting the bacterial growth, which indicated that ZNs inhibited the QS signaling regulated by *N*-acyl homoserine lactone. ZN2 had a higher inhibitory action on the virulence factor productivity than ZN1. Furthermore, ZN2-treated cells displayed a substantial decrease in azocasein-degrading protease activity (80%), elastase activity (83%), and pyocyanin production (85%) relative to untreated *P. aeruginosa* PAO1 cells. Treatment with ZN2 decreased swarming motility and exopolysaccharide production by 89 and 85%, respectively. ZN2 was effective against both the *las* & *pqs* systems of *P. aeruginosa* and exhibited broad-spectrum activity. Additionally, ZN2 was more efficient in inhibiting the biofilm formation at the attachment stage than ZN1. These findings revealed that in *P. aeruginosa*, ZN2 demonstrated inhibitory effects on QS as well as on the development of biofilms. Thus, ZN2 can be potentially used to treat drug-resistant *P. aeruginosa* infections.

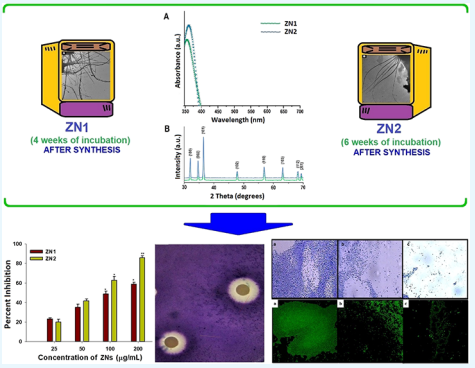

INTRODUCTION

Irrational and sustained application of antibiotics has culminated in the proliferation of multidrug-resistant (MDR) bacteria, which are associated with both hospital-acquired and community-acquired infections. Combating MDR bacterial infections is challenging because of the ineffectiveness of currently used antibiotics and slow development of novel antibiotics.[1] Hence, there is a renewed scientific interest in developing alternative antimicrobial strategies, such as antivirulence therapy. In contrast to the antibiotic treatment that involves killing the pathogen, the antivirulence technique is based on inactivating the pathogen by inhibiting its virulence factors,[2] thus reducing the probability of the pathogens developing resistance to this line of attack.[3] The current thrust areas in antivirulence therapy include quorum sensing (QS) inhibition[4,5] and biofilm formation.[6,7]

Pathogenic bacteria such as *Pseudomonas aeruginosa* regulate their pathogenicity, virulence factor production, and biofilm formation via QS.[8] *P. aeruginosa* is an infectious opportunistic bacteria, primarily causing nosocomial infections, which leads to mortality in immune-compromised patients.[9] In *P. aeruginosa*, *N*-acyl homoserine lactones (AHLs) activate the QS signaling, which is regulated by three frameworks: las, rhl, and pqs systems[10] that are interlinked by intracellular signaling molecules (autoinducers) and *Pseudomonas* quinolone-based signal (PQS), provided by the bacterial cells. These QS systems control the generation of virulence factors *viz.* elastase, exotoxins, exoproteases, pyocyanin, rhamnolipid, pyoverdin, and siderophores; all involved in the formation of biofilms.[11] Compared with the planktonic form, *P. aeruginosa* biofilms have higher antibiotic resistance. Thus, it is a very challenging to treat biofilm-based infections.[12] The groundbreaking detection of halogenated furanones from marine algae *Delisea pulchra* as QS inhibitor (QSI)[13] ushered the scientific community toward discovering new natural and synthetic QSIs.[14] Some natural QSIs from edible plants such as resveratrol[15] are nontoxic; however, a few furanones exhibit a

Received: July 29, 2020
Accepted: November 4, 2020
Published: December 10, 2020

https://dx.doi.org/10.1021/acsomega.0c03634
ACS Omega 2020, 5, 32203−32215

certain level of toxicity to humans and are unstable.[16,17] Thus, there is an increased effort on developing nanoparticles (NPs) that target QS and biofilm formation in the pathogens without harming the host.[18]

Metal and metal oxide NPs are now widely used for several medical and pharmaceutical applications. One of the promising metal nanomaterials is zinc (Zn) and its oxide (ZnO). Zinc is a highly active element with potent reducing properties; therefore, it can readily oxidize to form ZnO that can be exploited in the synthesis of ZnO-based NPs. Due to its distinctive optical, piezoelectric to semiconductor properties, ZnO has been studied in nanoelectronic/nano-optical devices and functions as energy storages/nanosensors.[19] Doping with suitable elements changes the optical properties of ZnO nanomaterials that can be used for bioimaging and delivery of drugs or genes.[20] They also display good protein adsorption properties and can therefore be used in the metabolism of human body systems, cytotoxicity regulation, and other cellular responses.[21] Due to the decreased toxicity, the US Food and Drug Administration (US FDA) has deemed ZnO as Generally Recognized As Safe or GRAS substances (21CFR182.8991).[22,23] Consequently, this makes it safe to be used on humans.

Numerous recent reports have analyzed the antibacterial effect of nanosized ZnO.[20,24−26] However, limited studies have evaluated the inhibitory effect of ZnO-based NPs on QS and biofilm formation. Previously, we established significant antimicrobial activity for thorn-like ZnO NPs.[26] In this study, we synthesized ZnO nanospikes (ZNs) using the sol−gel approach at ambient conditions. The effect of incubation periods on the morphologies of ZNs was also evaluated. Two Gram-negative bacteria namely *Chromobacterium violaceum* (strains 12472 and CVO26) and *P. aeruginosa* (PAO1) were assessed for the inhibitory effect of ZNs on QS-monitored virulence factor production and biofilm growth. Treatment with ZNs reduced lasA protease, lasB elastase, pyocyanin production, and biofilm formation. ZNs demonstrated widespread antibacterial activities and was efficient against the *P. aeruginosa las* and *pqs* systems. Additionally, ZN2 was more effective in the inhibition of the biofilm formation at the attachment stage than ZN1. This is the first study, according to the literature survey, to assess the anti-QS behavior of the subinhibitory compositions of ZNs synthesized at different incubation times.

RESULTS AND DISCUSSION

Several studies have reported that QS can be potentially targeted to combat the pathogenic bacteria.[27,28] Halogenated furanones are known to successfully interfere with AHL and suppress bacterial QS. However, the existing halogenated furanones are very reactive and hence apparently toxic for treating bacterial infections in humans.[29] Additionally, at subinhibitory concentrations, some furanones have shown to enhance biofilm formation.[16] In recent years, researchers utilize nanotechnology to develop next-generation nano-antimicrobials that can target QS and virulence factors, without affecting the mammalian cells. Moreover, these nanomaterials exhibit several advantages, such as higher solubility, better biofilm penetration, effective delivery, and maintenance of the activity of QSIs.[30] The anti-QS and the biofilm inhibitory properties of silver (Ag) NPs/nanocomposites have been well established.[3,31,32] Here, we report the anti-QS property of ZnO NPs synthesized under different incubation conditions.

Characterization of ZNs. Earlier, we developed flower-shaped ZnO NPs at various temperatures using a simple sol−gel synthesis process, while avoiding sophisticated equipment.[33] Our group also reported the mechanical stirring effect on ZnO NP synthesis, which exhibited thorn-like morphology.[26] In this study, we report the diversified growths of ZnO NPs in the form of nanospikes (ZNs) of distinct aspect ratios (L/D; length by diameter), fabricated at two different incubation conditions. The ZNs (ZN1 and ZN2) were prepared at ambient temperature as it was reported that NPs synthesized at near-room temperature displayed better activity against microbes.[33] The transmission electron microscopy (TEM) study revealed the overall surface morphology of the ZN1 and ZN2 structures (Figure 1A,B). The ZNs were found

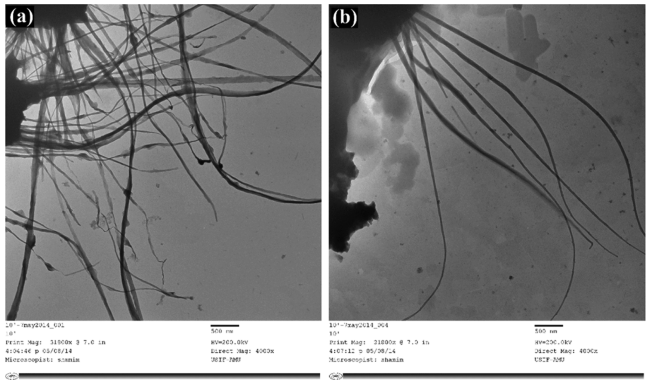

Figure 1. Size and shape characterization: TEM micrographs of ZNs kept under different incubation periods: (A) 4 and (B) 6 weeks.

to be spike-like in nature, with long thread-shaped structures stretching up to several micrometers in length. The average diameter size of ZNs was in the range of 40−130 nm. The growth and the sharpness of the nanoparticles were directly proportional to the incubation period. An increase in the incubation period resulted in the formation of finer particles. Longer incubation time expedites proper mixing and better dispersion with the surfactant, cetyltrimethyl ammonium bromide (CTAB) (along with the ion carriers), on a predetermined pH, leading to the unified growth of ZNs toward the geometry of a specific facet ⟨0 0 0 1⟩, that is, length (c-axis), while decreasing its cross-sectional area; thus changing the aspect ratio. Several previous studies have highlighted that different parameters such as time, temperature, kinetic energy barrier, and capping molecules exert control over the nanocrystal growth pattern under different conditions.[33−35] Cozzoli and Manna[36] discussed that the surfactant-supported chemical−assist reactions allowed facile growth to varied shapes and sizes of semiconductors, oxides, and metal nanocrystals by balancing different parameters. Moreover, in literature, diverse preparation techniques such as sol−gel method,[26] solution precipitation method,[37] spray pyrolysis,[38] hydrothermal method,[34] microwave-assisted technique,[39] and water-assisted synthesis[40] have resulted in various structures and forms of ZnO NPs such as nanothorns,[26] nanorods,[37] hexagonal,[38] nanoflowers,[34] microspheres,[39] and nanoprisms,[40] respectively.

The optical property of ZNs was characterized by UV−vis absorption spectroscopy. A strong, narrow, and sharp band of absorption was obtained around 350−380 nm (existing in the UV-B region), which was free from any other peak points. This

https://dx.doi.org/10.1021/acsomega.0c03634
ACS Omega 2020, 5, 32203−32215

peak is an important and typical value of characterization for absorption of the pure hexagonal wurtzite ZnO structure (Figure 2A).[26] Furthermore, absorption peak intensity was

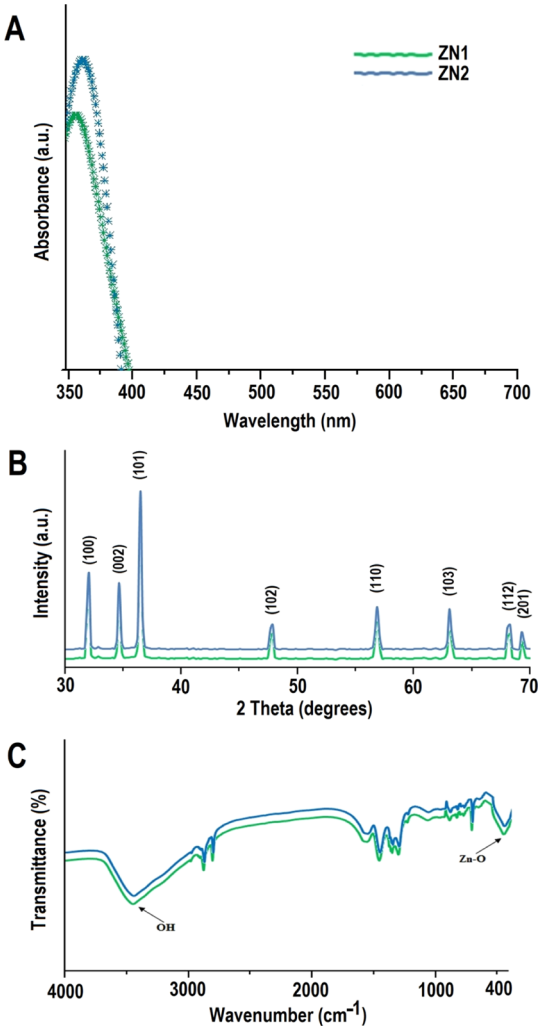

Figure 2. Characterization of ZNs: (A) UV−vis spectra, (B) XRD, and (C) FTIR spectra of ZNs prepared under different incubation periods.

observed to be elevated at higher incubation period (6 weeks). A small shift in the λ_{max} of the absorption spectra of the ZNs was also observed when incubation time was increased from 4 to 6 weeks. This hypsochromic shift in λ_{max} of ZNs at higher incubation period was due to the decrease in the aspect ratio of ZNs and thereby concomitantly increase in the absorbance was observed. Our results are in agreement with previous reports which indicated that the shifting of the peak is determined by crystal size, reaction temperature, solvent used, mode of synthesis, and the maturation time of samples.[41−43]

An X-ray diffraction (XRD) pattern was used to analyze the phase and crystal parameters of synthesized ZN1 and ZN2 samples (Figure 2B). The nature of the peaks depict the smaller size and crystalline nature of the synthesized ZN samples. The strongest peak at $2\theta = 36.2°$ was obtained along the (101) orientation.[26] Moreover, the peaks obtained at planes (100), (002), (102), (110), and (103) suggested the pure wurtzite structure of ZnO, as mentioned in The International Centre for Diffraction Data (ICDD, USA card no. 080-0075). No peaks other than the standard peak were observed, which suggested that the synthesized ZN samples were pure. After 4 and 6 week incubation time, average size of the particles was estimated to be ∼50 and ∼115 nm, respectively, when applying the Debye−Scherrer formula (from dominant peak based on the full width at half maximum, FWHM), which implies that both peak widths and crystal sizes are inversely linked.

ZnO is known to occur in three crystal (lattice) structures *viz.* rock-salt (B_1), cubic zinc-blende (B_3), and wurtzite (B_4).[44,45] The zinc-blende shape is stabilized by hetero-epitaxial expansion on cubic substrates, for example GaAs/ZnS, ZnS, and Pt/Ti/SiO_2/Si, while the structure of the Rochelle salt/rock salt (NaCl) is a metastable state reached at high pressure only. Wurtzite ZnO is a hexagonal crystal having lattice parameters "*a*" and "*c*" and a lattice constant (c/a) of $\sqrt{8/3}$ (1:633, in a typical wurtzite hexagonal structure), with [0 0 0 1] or basal plane as the surface most frequently used for growth.[46] This structure is part of the space group C^4_{6v} in the Schoenflies notation and $P6_3mc$ in the Hermann−Mauguin system and exhibits a noncentrosymmetric structure (a condition at where the space groups lack inversion center).[46] At ambient conditions, only the wurtzite structure has a thermodynamically stable hexagonal unit cell,[44] wherein four oxygen atoms surround each tetrahedral Zn atom and *vice versa*[47]

The Fourier transform infrared (FTIR) spectroscopy analysis of ZNs was performed in the range of 400−4000 cm^{-1} at room temperature (Figure 2C). In general, metal oxides display absorption bands below 1000 cm^{-1} in the fingerprint region, which is generated by inter-atomic vibrations. The peculiar absorption band of the Zn−O stretching vibration mode was around 373 cm^{-1}[48] that corresponds with the hexagonal ZnO wurtzite E_2 form. The other characteristic vibration modes were of O−H (around 3465 cm^{-1}), C−O (around 1140 cm^{-1}), and C═O (around 1450 cm^{-1}).[26] In ZN samples, the peaks observed at 1520.23 and 1450.14 cm^{-1} corresponded to the asymmetric and symmetric stretching vibrations of the C═O functional group.[49] Previous studies documented two separate interactions of O−H groups on the surface of the ZNs:[50] (i) 1610−1630 cm^{-1} band attributable to the H−O−H vibration bands of chemisorbed water bending[51] and (ii) 3000−3650 cm^{-1} band corresponding to Zn and O reversible dissociative hydrogen absorption.[52] The peak around 760 cm^{-1} can be accredited to the stretching of the C−O bond. These results show that even under different stirring conditions, the ZnO NPs preserved their structures. Similar peaks were observed for thorn-like ZnO NPs,[26] albeit with the difference of a new peak (at 1140 cm^{-1}) observed in our case.

Minimum Inhibitory Concentrations. Minimum inhibitory concentrations (MICs) of ZN1 versus *C. violaceum* (CV12472 and CVO26) and *P. aeruginosa* (PAO1) were found to be 512, 512, and 800 μg/mL. In the same way, MICs of ZN2 were shown to be 400 μg/mL against all test pathogens (Table 1). Concentration levels below MICs (sub-MICs) have further been used to determine the ZNs' inhibitory properties on QS and formation of biofilms. Several studies involving metal oxide NPs have reported the MIC value of 256 μg/mL (for Ag-NPs)[53] and 500 μg/mL (for zinc NPs)[54] against *P. aeruginosa*.

Anti-QS Activity of ZNs. Biosensor *C. violaceum* strain CV12472 was used to screen the potent inhibitory effects of

https://dx.doi.org/10.1021/acsomega.0c03634
ACS Omega 2020, 5, 32203−32215

Table 1. Antimicrobial Activity of ZNs at Different Incubation Periods

Organism	MIC (μg/mL)	
	ZN1	ZN2
C. violaceum CV12472	512	400
C. violaceum CVO26	512	400
P. aeruginosa PAO1	800	400

the synthesized ZNs on QS. The production of violacein, a violet colored pigment, is regulated by the QS that depends on *CviI/R* AHL system. Consequently, inhibition of pigment formation indicates the interaction with AHL-regulated QS.[55] Both ZN1 and ZN2 dose-dependently decreased the violacein production. Additionally, the highest zone of pigment inhibition by ZN1 and ZN2 was observed at a concentration of 200 μg/mL (Figure 3A).

The quantification of inhibition of violacein formation was carried out by extracting violacein from the biosensor *C. violaceum* CVO26 strain treated with sub-MICs of ZNs. The colorimetric study showed that ZNs significantly decreased the production of violacein in *C. violaceum* CVO26 at various concentrations. ZN1 at sub-MICs (25, 50, 100, and 200 μg/mL) decreased violacein production by 28, 40, 52, and 65%, respectively. Similarly, ZN2 inhibited AHL-regulated violacein production in a dose-dependent manner. The production of violacein decreased by 30−92% upon treatment with ZN2 (Figure 3B). At the highest ZN concentration (200 μg/mL), no significant difference in the cell densities of CVO26 was observed (Figure 3C). These results demonstrate that the ZNs interfered with AHL-regulated QS signaling, inhibiting the production of violacein, without effecting the growth of the bacteria. The findings are consistent with a study on anti-QS properties of NPs, wherein an 80% reduction in violacein production was observed at a 4 mg/mL concertation.[56] Some other studies have reported that the nanostructures decreased violacein production by ∼90%.[55,57]

Virulence Factors Inhibition by ZNs. The growth kinetics analysis of *P. aeruginosa* strain PAO1 showed that the pathogen cell density was not significantly affected upon treatment with 200 μg/mL of ZNs (Figure 4A). This indicated that the synthesized NPs did not reduce the growth of the *P. aeruginosa* as well, consistent with the result obtained in the case of biosensor *C. violaceum* CVO26 strain (Figure 3C).

Various types of virulence factors are produced by *P. aeruginosa* in a synchronized manner for host colonization and adaptation.[58−60] These include elastase, pyocyanin, rhamnolipid, and biofilm production.[11,61] Extracellular protease (lasA) and elastase (lasB) are believed to play key roles in *P. aeruginosa* infection[62] by degrading the host tissue enabling systemic spread of the pathogen. Coordinated expression of these proteases is very important for successful infection, and QS is considered to be a mechanism to enable this. Another significant redox active small-molecule QS-regulated virulence factor is pyocyanin, which is documented to play a significant role in the pathogenesis, because it damages the host neutrophil-mediated protection system.[63] Interfering with the QS system through application of QSI is, therefore, a potential antivirulence strategy to effectively reduce virulence in *P. aeruginosa* infections.[63] Thus, the impacts of ZN1 and ZN2 sub-MICs on QS managed virulence factors such as total protease, elastase, pyocyanin generation, swarming motility, and exopolysaccharide (EPS) development in *P. aeruginosa* PAO1 were evaluated in this study. ZN1 dose-dependently

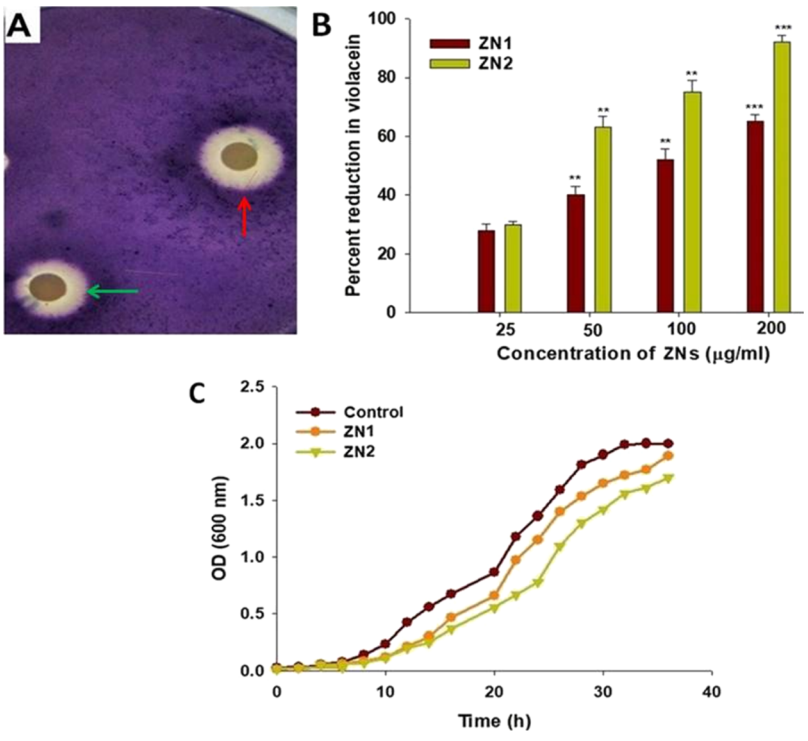

Figure 3. Assay for QS inhibition: (A) screening for anti-QS activity using *C. violaceum* 12472 biosensor strain. The figure shows zone of pigment inhibition, green arrow (ZN1) and red arrow (ZN2). (B) Analysis of the growth curve of *C. violaceum* CVO26 at a concentration of 200 μg/mL of ZN. (C) Inhibition of violacein production in CVO26 by different ZN (ZN1 and ZN2) concentrations (25−200 μg/mL), as quantified spectrophotometrically at 585 nm.

https://dx.doi.org/10.1021/acsomega.0c03634
ACS Omega 2020, 5, 32203−32215

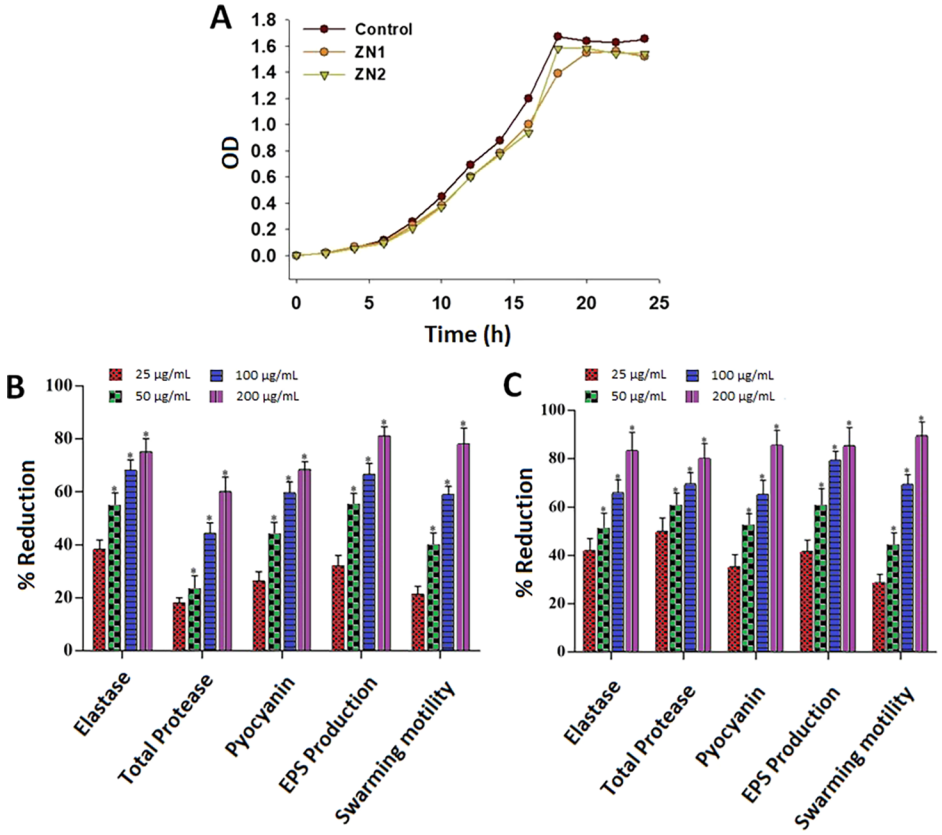

Figure 4. QS-regulated virulence traits of PAO1: (A) analysis of the growth curve of *P. aeruginosa* PAO1 incubated with ZN at a 200 μg/mL concentration. Effects of sub-MICs of (B) ZN1 and (C) ZN2 on inhibition of the QS-regulated virulence factor. Data are expressed as mean % reduction ± SD. *≤ 0.05, **≤ 0.005, and ***≤ 0.001 vs control.

decreased the production of elastase (35−74%), total protease (17−58%), and pyocyanin (25−67%) at concentrations ranging from 25 to 200 μg/mL (Figure 4B). The inhibition of virulence factor production by ZN2 was higher than that by ZN1 over the same concentration range. Treatment with 200 μg/mL of ZN2 significantly reduced azocasein-degrading protease activity (80%), elastin degrading elastase activity (83%), and pyocyanin production (85%) in *P. aeruginosa* PAO1, as compared to the control (Figure 4C). Prateeksha et al.[64] reported a 52 and 60% decrease in elastase and protease production respectively, after treatment with selenium nanovectors at sub-MIC. In case of *Terminalia chebula* extract, a similar decline in the development of pyocyanin was observed.[65] Our findings, therefore, showed that ZN decreased elastase and pyocyanin production in *P. aeruginosa* strains, consistent with the previously published reports.[66,67]

Exopolymeric materials play a key role in the maintenance of biofilm architecture and provide the scaffold for adhesion to surfaces and cohesion between cells, offering increased resistance against antibiotics and host immune defenses, as well as to osmotic and oxidative stresses.[68] *Pseudomonas* also display a multicellular swarming motility on semi-solid surfaces, which involves substantial alterations in metabolic processes and gene expression, and thus, results in increased resistance to several antibiotics.[69,70] Moreover, swarming motility of flagellar and pili regulated by QS is a kind of virulence factors due to its association with the cell/surface attachment during biofilm development.[71,72] Hence, reduced EPS development and attenuated swarming motility contribute to impaired biofilm formation, which increases drug sensitivity of pathogens and makes them susceptible to the host immune system. The results of this study indicated that the sub-MICs (25−200 μg/mL) of ZNs can inhibit EPS production in *P. aeruginosa* PAO1. Furthermore, ZNs reduced the swarming migration of the target organism. Treatment with ZN1 diminished the production of EPS by 30−79% and decreased the swarming motility by 22−78%, as compared to the untreated control (Figure 4B). Similarly, treatment with ZN2 significantly inhibited the production of EPS and swarming migration at various concentrations. ZN2 reduced the production of EPS by 41−85% as well as the motility of *P. aeruginosa* PAO1 by 28−89% (Figure 4C). Various plant extracts such as *Cuminum cyminum*,[71] *Mangifera indica*,[72] *Alpinia officinarum*,[70] and *Cinnamomum tamala*[70] as well as secondary metabolites,[73,74] green tea,[75] and essential oils[67,76] have been reported to hinder the swarming motility of *P. aeruginosa* PAO1. However, there are limited studies that have evaluated the effect of metal NPs on the attenuation of swarming motility. Intrinsically, sub-lethal concentrations of tin oxide hollow nanoflowers[77] as well as silver[78] and gold[79] NPs demonstrated major inhibition of the mobility of *P. aeruginosa* PAO1, suggesting biofilm interruption, which is in well-agreement with our data.

***β*-Galactosidase Activity Assay.** The expression of QS-regulated genes that encode virulence factors (like *lasB* and *pqsA*) of *P. aeruginosa* PAO1 was investigated for the analysis of ZNs anti-QS activity. A *β*-Galactosidase assay was performed to determine the impact of ZNs (25−200 μg/mL) on the transcriptional function of *lasB* and *pqsA*. ZN1 and ZN2 respectively decreased the transcriptional activity of *lasB*

https://dx.doi.org/10.1021/acsomega.0c03634
ACS Omega 2020, 5, 32203−32215

Table 2. Effect of ZNs on Transcriptional Activity of lasR and pqsA

	ZN1		ZN2	
Concentration (μg/mL)	lasR	pqsA	lasR	pqsA
control	1452 ± 22.3	967 ± 34.7	1452 ± 22.3	967 ± 34.7
25	1336 ± 14.6	808 ± 26.4	1380 ± 18.7	763 ± 41.2
50	1162 ± 25.8	681 ± 39.6	930 ± 41.2	579 ± 45.8
100	973 ± 31.7	553 ± 44.5	711 ± 29.1[a]	461 ± 38.7[a]
200	653 ± 26.7[a]	474 ± 27.3[a]	552 ± 38.7[b]	425 ± 34.4[a]

[a] $p < 0.05$. [b] $p < 0.005$.

by 45 and 62%. Similarly, at a concentration of 200 μg/mL, ZN1 and ZN2 decreased the transcriptional activity of *pqsA* by 51 and 56%, respectively (Table 2). A previous study found that the regulation of lasB-lacZ expression is sensitive to the concentration of autoinducers.[80] The findings of our study are consistent with the above observation. ZN1 and ZN2 treatment decreased the activity of β-galactosidase, which indicated diminished levels of AHL, and thus are suggestive of downregulation of *lasB* gene expression.

PQS, also called as 2-heptyl-3-hydroxy-4-quinolone, has been revealed to regulate the expression of multiple virulence factors in *P. aeruginosa*.[81] The PQS signal is intertwined with the QS cascade, acting as a regulatory link between the QS systems *las* and *rhl*.[82,83] The development of pyocyanin in *P. aeruginosa* strain PAO1 is also mainly regulated by the *pqs* system.[84] The inhibition of the *pqs* system, thus, may disrupt quinolone signaling in *P. aeruginosa,* and the downregulation of these genes may interfere with the normal production of various virulence factors, *viz.* lasA protease, lasB elastase, rhamnolipid, and pyocyanin through the activity of lasAB and phzA1 operons, respectively. Our study revealed that ZNs decreased the transcriptional activation of *pqsA* and inhibited the *pqs* system. Consequently, the findings of this assay demonstrate the wide spectrum anti-QS property of ZN due to its inhibition of both *las* and *pqs* systems.

Effect of ZNs on Cell Attachment. The first stage in the formation of biofilms is cell attachment to a surface followed by its assembly to form microcolonies and finally differentiation of biofilms into a mature structure.[85] It has been suggested that biofilm formation might be prevented by inhibiting initial adhesion. Furthermore, a previous study has proved that the inhibition of preformed biofilm development is more complicated to achieve as compared to the cell attachment phase.[86] Therefore, the antiattachment property of ZNs against *P. aeruginosa* PAO1 was evaluated. The synthesized NPs significantly inhibited cell attachment to the microtiter plate. Compared to the control, treatment with 25, 50, and 100 μg/mL of ZN1 inhibited the cell attachment by 23, 35, and 48%, respectively.

Similarly, treatment with 25, 50, and 100 μg/mL concentration of ZN2 inhibited the cell attachment by 20, 41, and 62%, respectively, as compared to the control (Figure 5). ZN1 and ZN2 at a concentration of 200 μg/mL inhibited cell attachment by 58 and 85%, respectively. These results indicate that the NPs inhibit biofilm at the attachment stage and can be used as coatings on surfaces to prevent cell attachment and hence prevent biofilm formation. Similar results have been reported by other authors.[56,77]

Inhibition of ZNs on Biofilm Formation. QS plays a crucial role in the production of biofilms, which are used by pathogenic bacteria to activate virulence and develop antibiotic resistance.[87] Therefore, the deactivation of QS can be a

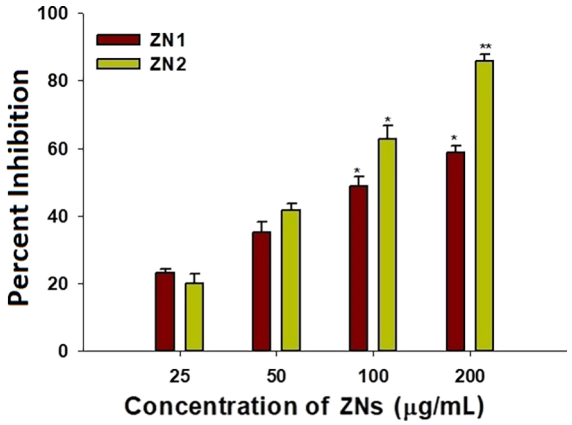

Figure 5. Effect of sub-MICs of ZNs on *P. aeruginosa* PAO1 biofilm attachment, presented as percentage inhibition.

preventive strategy for biofilm formation in *P. aeruginosa* PAO1. Microscopic analysis of biofilm inhibition showed reduction in the number of micro-colonies (Figure 6A). Images of confocal laser scanning microscopy confirmed the light microscopy results as key interruption in the biofilm architecture of *P. aeruginosa* strain PAO1 was observed (Figure 6B). ZN1 reduced biofilm formation by 23−58% in a concentration-dependent manner. ZN2 was found to be more potent in biofilm inhibition at greater concentrations as compared to ZN1. Treatment with 25, 50, 100, and 200 μg/mL of ZN2 impaired the formation of biofilm by 20, 41, 62, and 85%, respectively, when compared to untreated control (Figure 6C).

Biofilms are complex, immobile microbial communities having various types of bacterial colonies or single type of cells in a group that adhere to the surface.[88] Cells residing in biofilms are approximately 1000 times more resistant to their planktonic forms.[12] Biofilm-associated *P. aeruginosa* diseases are becoming problematic to treat due to the rise in the MDR and persistent biofilm infections.[89] Therefore, a biofilm is a potential drug target against drug-resistant microorganisms. In this study, treatment with ZN1 and ZN2 significantly decreased the biofilm biomass. This is in conformity with the results of previous studies, which reported that zinc oxide,[56,90] tin oxide,[77] iron oxide,[91] and silica NPs[92] as well as agents, such as doxycycline[93] and ceftazdime[84] inhibit *P. aeruginosa* biofilm formation. Moreover, the disruption of the QS system with furanones has also been reported to reduce biofilm growth.[17] Decreased biofilm formation could be due to reduced swimming motility as flagella-mediated motility is caused to promote biofilm formation by initiating cell to surface attachment. A previous study has also reported a similar kind of effect using phenylacetic acid, which inhibited

https://dx.doi.org/10.1021/acsomega.0c03634
ACS Omega 2020, 5, 32203−32215

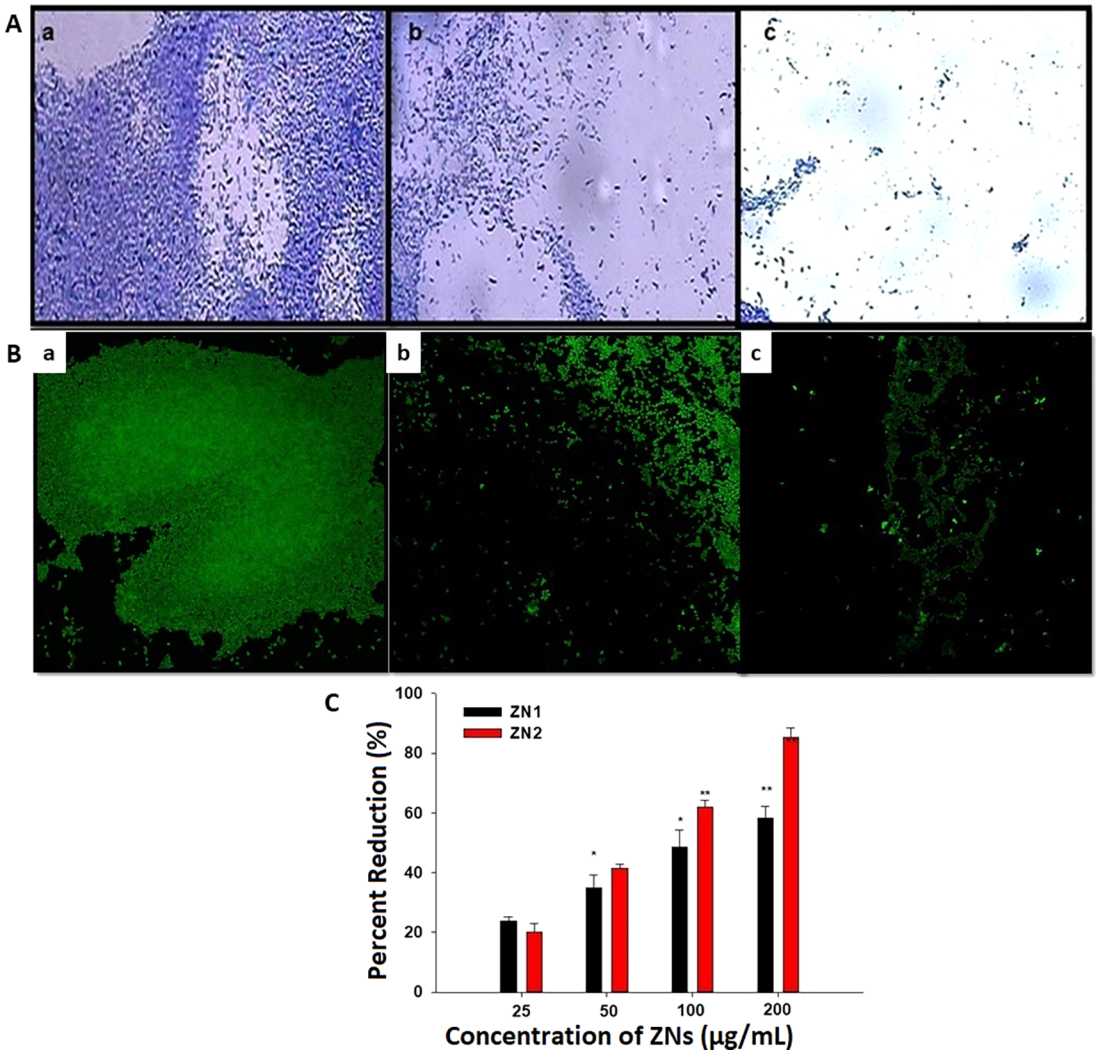

Figure 6. Anti-biofilm activity of ZNs: (A) images of *P. aeruginosa* biofilm (a–c) CV staining under a light microscope, (B) acridine orange staining under a confocal laser scanning microscope. (a) Control, untreated, (b) 200 μg/mL of ZN1, and (c) 200 μg/mL of ZN2. (C) Effect of sub-MICs of ZN1 and ZN2 on percent inhibition of biofilm formation of *P. aeruginosa* PAO1.

the biofilm formation by interfering with swimming motility of *P. aeruginosa*.[94]

CONCLUSIONS

This study encompasses the synthesis of discrete ZNs, prepared at different incubation periods (4 and 6 weeks). The diameter of the synthesized nanospikes was found to be in the range of 40–130 nm; with finer particles synthesized at a longer incubation period of 6 weeks. The present investigation also highlights the inhibitory effect of ZNs on QS and biofilm formation, which can enhance the antibiotic efficiency and decrease the pathogenicity of bacterial pathogens that can be exploited in the future for the treatment of drug-resistant infections of *P. aeruginosa*. Furthermore, these findings confirm the positive effect of increased incubation period on the activity of ZNs as NPs synthesized at a longer incubation period were found to be more active than those synthesized at a shorter incubation period.

EXPERIMENTAL SECTION

Chemicals. All analytical grade chemicals were obtained (with no extra purification) from Merck Limited, India. For the synthesis of ZNs, double-distilled water (DDW) was used. All glassware were purchased from Borosil, India.

Bacterial Strains and Growth Conditions. Violacein, a QS-regulated purple pigment, is produced by *C. violaceum* wild strain 12472 in response to cognate C_4 and C_6 AHLs. However, *C. violaceum* CVO26, a violacein and AHL-negative double mini Tn5 mutant, generates violacein in the presence of short-chain auto-inducers. *P. aeruginosa* strain PAO1 is an opportunistic pathogen in which several virulence factors and traits are regulated by QS. All pathogenic strains were maintained on Luria Bertani (LB) broth which comprises 0.5% yeast extract, 15.0% tryptone, and 0.5% NaCl salt. LB broth was used to prepare LB agar by adding 1.5% agar (Hi-media). The *C. violaceum* 12472 and *C. violaceum* CVO26 strains were cultured at 28 °C, whereas *P. aeruginosa* PAO1 was cultured at 37 °C.

Synthesis of ZNs. ZNs were synthesized at ambient temperature using DDW by two different reactant conditions. In synthesis—A, 10 mL solution of 0.1 M zinc acetate dihydrate was mixed with 160 mL of DDW using a magnetic stirrer. Next, 0.001 mol of a capping agent, CTAB, was added to the solution under constant stirring. The reaction was then terminated by gradually adding >0.5 g of sodium hydroxide, an

https://dx.doi.org/10.1021/acsomega.0c03634
ACS Omega 2020, 5, 32203–32215

ion carrier, to the mixture. The reaction mixture was incubated for less than an hour until a white cloudy appearance was observed. The solution was then transferred to the centrifugation tubes and incubated at ambient temperature for 4 weeks. Finally, the product was washed with the help of DDW and 99.8% absolute alcohol. This sample was labeled as ZN1 and stored for further characterization. In synthesis—B, the same procedure was repeated, except for the incubation condition, which was 6 weeks at ambient temperature. Finally, the product was washed with DDW and 99.8% absolute alcohol, labeled as ZN2, and stored for further studies.

Characterization of ZNs. The XRD analysis of ZNs was examined using an X-ray diffractometer (Bruker AXSD8 ADVANCE, Germany). The sample was exposed to Cu-K_α radiations of 1.54 Å wavelength, with the angular range of 30−70°. The diversified growths of the different ZN morphologies and their respective sizes were analyzed by the TEM instrument (JEOL JEM-2100, Japan). Moreover, the compositional quality of ZNs was analyzed by the FTIR spectrometer (Thermo Scientific Nicolet iS 10).

Calculation of MICs. The MICs of ZNs against the pathogenic bacteria were evaluated by the macro-broth dilution method.[56] The MIC was taken as the least concentration of ZN at which no observable growth of test pathogenic strains was observed. Therefore, the concentrations of the ZN samples below the MIC value were considered as sub-inhibitory, which were used to study the inhibitory effects of ZNs on QS and biofilm formation.

Inhibition of Violacein Production. A biosensor bioassay for violacein production by *C. violaceum* 12472 was evaluated using a disc diffusion assay, as descried earlier.[56] *C. violaceum* was grown overnight in LB broth. Then, 50 μL of the culture was added to 5 mL of molten soft LB agar (0.3% w/v) and immediately poured onto LB agar plates containing 5 μg/mL of C_6-AHL. ZNs at sub-MIC concentrations were applied on sterilized paper discs and placed on the surface of the agar medium. The plates were then incubated overnight at 30 °C and examined for violacein pigment production. A colorless, opaque zone of inhibition of violacein (loss of pigmentation) around the disc was considered as anti-QS activity.

Quantitative Estimation of Violacein. The extent of violacein production by *C. violaceum* (CVO26) in the presence and absence of sub-MICs of ZNs was studied by extracting violacein and quantifying photometrically using the method of Blosser and Gray[95], with slight modifications.[71] Briefly, *C. violaceum* CV026 biosensor strain was cultured for approximately 18 h. Next, the culture with an optical density of 0.1 at 600 nm (OD_{600}) was inoculated into LB medium supplemented with 10 μM C_6-HSL and ZNs in an Erlenmeyer flask. The flasks were incubated in a shaker at 27 °C and 150 rpm for 24 h. Afterward, 1 mL of fresh culture from each flask was subjected to centrifugation for 10 min at 13,000 rpm to obtain the insoluble precipitate of violacein. Furthermore, 1 mL of dimethyl sulfoxide was added to the pellet and mixed vigorously for 30 s to complete the solubilization. The cell debris was then removed by centrifuging the mixture at 13,000 rpm for 10 min. The supernatant containing violacein (200 μL) was transferred to a 96-well microplate (POLYLAB, India). The absorbance of the mixture was measured at 585 nm in a microplate absorbance reader (Thermo Scientific, Multiskan Ex., India). Finally, the percent inhibition of pigment production (in the presence of ZNs) was calculated as follows:

$$\frac{OD_{control} - OD_{treated}}{OD_{control}} \times 100$$

This experiment was carried out in quadruplets, and the results are well expressed as mean ± SD.

Effect of ZNs on the Production of the Virulence Factors. Effects of sub-MICs of ZNs on the production of virulence factors in *P. aeruginosa* (lasB elastase, protease, and pyocyanin), swarming motility, and EPS extraction and quantification were assessed following established methods, as described below.

(a) LasB Elastolytic Activity Assay. The lasB elastolytic activity was evaluated as per the method described previously.[96] The bacterial culture was treated with ZNs for 16 h at 37 °C. Then, 100 μL of both treated and untreated culture supernatant was incubated with 900 μL of elastin Congo Red (ECR) buffer (100 mM Tris, 1 mM $CaCl_2$, at pH 7.5) supplemented with 20 mg of ECR (Sigma, USA) for 3 h on a shaker at 37 °C. After centrifugation, insoluble ECR was decanted, and the absorption of supernatant containing Congo Red was evaluated at 495 nm. The culture-free LB medium with ZNs and without ZNs was considered as a negative control.

(b) Azocasein Degrading Proteolytic activity. Proteolytic action of cell-free supernatants of *P. aeruginosa* PAO1 cultured with and without ZNs at sub-MIC concentrations was determined using the published protocol.[97] Briefly, 150 μL each of culture supernatants were incubated with 1 mL of 0.3% azocasein (Sigma, USA) in 0.05 M Tris−HCl and 0.5 mM $CaCl_2$ (pH 7.5) at 37 °C for 15 min. Trichloroacetic acid (10%, 0.5 mL) was added to stop further reaction. The mixture was then centrifuged and the absorbance was recorded at 400 nm.

(c) Determination of Pyocyanin Level. The pyocyanin level was determined following the previously reported method.[98] A 5 mL of treated and untreated culture supernatant of *P. aeruginosa* PAO1 with ZNs was extracted with 3 mL of chloroform and then re-extracted with 1 mL of 0.2 M HCl for pink to deep-red colored solution development. Then, the extracted solution was used to read the absorbance at 520 nm.

(d) Swarming Motility Assay. Swarming motility of bacteria was assessed as mentioned earlier.[99] An overnight culture of *P. aeruginosa* PAO1 was inoculated at the center of the medium (1.0% tryptone, 0.5% NaCl, and 0.3% agar) with or without various sub-inhibitory concentrations *viz.* 25, 50, 1000, and 200 μg/mL of ZNs.

(e) EPS Extraction and Quantification. The test strain *P. aeruginosa* PAO1 cultured with or without ZNs was centrifuged, and the supernatant was filtered followed by incubation with three volumes of chilled absolute ethanol overnight at 4 °C to precipitate EPS.[99] EPS was quantified by measuring sugars, as per the previous protocol.[100]

***lasB* and *pqsA* Transcriptional Activity Analysis.** The transcriptional activities of *lasB* and *pqsA* in *Escherichia coli* MG4/pKDT17 and *E. coli* pEAL08-2 were analyzed using β-galactosidase assay, as mentioned previously.[80,101] Briefly, the QS signal molecules (AHLs) in the supernatant of overnight cultures of *P. aeruginosa* PAO1 grown in the presence or absence of sub-MICs of ZNs were extracted using ethyl acetate solvent. Next, 2 mL culture of reporter strains *E. coli* MG4 (pKDT17)/*E. coli* pEAL08-2 and 0.5 mL of the ethyl acetate extracted supernatant were incubated at 30 °C in a water bath for 5 h with 100 rpm rotation. The reporter cell cultures were

https://dx.doi.org/10.1021/acsomega.0c03634
ACS Omega 2020, 5, 32203−32215

centrifuged at 3200 *g* for 15 min, and the cell pellet was re-suspended in Z-buffer solution (0.05 M β-mercaptoethanol, 0.04 M $NaH_2PO_4{\cdot}H_2O$, 0.06 M $Na_2HPO_4{\cdot}7H_2O$, 0.01 M KCl, and 0.001 M $MgSO_4{\cdot}7H_2O$, at pH 7.0). Then, 1 mL of Z-buffer, 200 μL of chloroform, and 100 μL of 0.1% sodium dodecyl sulphate were added with 1 mL of the cell suspension to lyse the cells. The cell suspension was then treated with 0.4 mL of *O*-nitrophenol-β-D-galactopyranoside (dissolved in 4 mg/mL of phosphate-buffered saline). After yellow color development, reaction was then stopped using 1 mL of 1 M Na_2CO_3. Absorbance of reaction samples was read at 420 and 550 nm. Units of β-galactosidase were calculated using the formula:

$$\frac{OD_{420\ nm} - (OD_{550\ nm} \times 1.75) \times 1000}{time \times volume \times OD_{600\ nm}}$$

Cell Attachment Assay. A 100 μL of the standardized culture (1.0×10^6 cfu mL^{-1}) was incubated with 100 μL of ZNs in the 96-well microtiter plates (final volume, 200 μL). Sterile media was also added as an additional control to check the sterility of the experiment. The 96-well plates were then sealed with a sterile sealing tape and incubated further at 37 °C for 8 h for the cell attachment and biofilm development. After incubation, a crystal violet assay was performed in triplicates to assess biofilm biomass.[102]

Biofilm Inhibition Assay. A polyvinyl chloride biofilm formation assay was performed to investigate the effect of ZNs on biofilm formation, as per the following protocol.[103] The overnight cultures of *P. aeruginosa* strain PAO1 were resuspended in fresh LB medium with and without ZNs and incubated at 30 °C for 24 h. Biofilms formed in a microtiter plate were stained with crystal violet solution followed by solubilization of dye in ethanol. Biomass was then quantified by measuring the absorbance at 470 nm.

Statistical Analysis. In the study, various experiments were carried out in triplicates. The data were presented as mean values. For statistical analysis, student's *t*-test was performed between control and test values.

AUTHOR INFORMATION

Corresponding Authors

Fohad Mabood Husain − *Department of Food Science and Nutrition, College of Food and Agriculture Sciences, King Saud University, Riyadh 11451, Saudi Arabia*; Phone: +966-502698271; Email: fahadamu@gmail.com

Qamar Zia − *Health and Basic Science Research Centre, Majmaah University, Majmaah 11952, Saudi Arabia; Department of Medical Laboratory Sciences, College of Applied Medical Sciences, Majmaah University, Majmaah 11952, Saudi Arabia*; orcid.org/0000-0002-0284-4974; Phone: +966-506798372; Email: qamarzia@mu.edu.sa

Authors

Mohd. Farhan Khan − *Nano Solver Lab, Department of Mechanical Engineering, Z. H. College of Engineering & Technology, Aligarh Muslim University, Aligarh 202002, India; Department of Science, Gagan College of Management and Technology, Aligarh 202002, India*

Ejaz Ahmad − *Interdisciplinary Biotechnology Unit, Aligarh Muslim University, Aligarh 202002, India*

Azfar Jamal − *Health and Basic Science Research Centre, Majmaah University, Majmaah 11952, Saudi Arabia; Department of Biology, College of Science, Majmaah University, Majmaah 11952, Saudi Arabia*

Mohammed Alaidarous − *Health and Basic Science Research Centre, Majmaah University, Majmaah 11952, Saudi Arabia; Department of Medical Laboratory Sciences, College of Applied Medical Sciences, Majmaah University, Majmaah 11952, Saudi Arabia*

Saeed Banawas − *Health and Basic Science Research Centre, Majmaah University, Majmaah 11952, Saudi Arabia; Department of Medical Laboratory Sciences, College of Applied Medical Sciences, Majmaah University, Majmaah 11952, Saudi Arabia; Department of Biomedical Sciences, Oregon State University, Corvallis, Oregon 97331, United States*

Md. Manzar Alam − *Regional Research Institute of Unani Medicine (Under CCRUM, Ministry of AYUSH), Patna 800008, India*

Bader A. Alshehri − *Health and Basic Science Research Centre, Majmaah University, Majmaah 11952, Saudi Arabia*

Mohd. Jameel − *Department of Zoology, Faculty of Life Sciences, Aligarh Muslim University, Aligarh 202002, India*

Pravej Alam − *Department of Biology, Prince Sattam bin Abdulaziz Univrsity, Alkharj 11942, Kingdom of Saudi Arabia*

Mohd Imran Ahamed − *Department of Chemistry, Aligarh Muslim University, Aligarh 202002, India*

Akhter H. Ansari − *Nano Solver Lab, Department of Mechanical Engineering, Z. H. College of Engineering & Technology, Aligarh Muslim University, Aligarh 202002, India*

Iqbal Ahmad − *Department of Agricultural Microbiology, Faculty of Agricultural Sciences, Aligarh Muslim University, Aligarh 202002, India*

Complete contact information is available at: https://pubs.acs.org/10.1021/acsomega.0c03634

Author Contributions

△M.F.K., F.M.H., and Q.Z. equal contribution.

Notes

The authors declare no competing financial interest.

ACKNOWLEDGMENTS

The authors are very grateful to the grant support of DST (New Delhi, India) under Project no. SR/NM/NS/91-2008. The authors are very thankful to Deanship of Scientific Research at the Majmaah University for providing the facilities. The authors acknowledge the Deanship of Scientific Research and Research Centre, College of Food and Agricultural Sciences, King Saud University, Riyadh, KSA for funding this research.

REFERENCES

(1) Aslam, B.; Wang, W.; Arshad, M. I.; Khurshid, M.; Muzammil, S.; Rasool, M. H.; Nisar, M. A.; Alvi, R. F.; Aslam, M. A.; Qamar, M. U.; Salamat, M. K. F.; Baloch, Z. Antibiotic Resistance: A Rundown of a Global Crisis. *Infect. Drug Resist.* **2018**, *11*, 1645−1658.

(2) Fleitas Martínez, O.; Cardoso, M. H.; Ribeiro, S. M.; Franco, O. L. Recent Advances in Anti-Virulence Therapeutic Strategies With a Focus on Dismantling Bacterial Membrane Microdomains, Toxin Neutralization, Quorum-Sensing Interference and Biofilm Inhibition. *Front. Cell. Infect. Microbiol.* **2019**, *9*, 74.

(3) Husain, F. M.; Khan, M. S.; Ahmad, I.; Khan, R. A.; Al-Shabib, N. A.; Oves, M.; Contreras, R. G.; Khan, M. S.; Arshad, M.; Alyousef,

A. A. Nanomaterials as a Novel Class of Anti-Infective Agents That Attenuate Bacterial Quorum Sensing. In *Antibacterial Drug Discovery to Combat MDR*; Ahmad, I., Ahmad, S., Rumbaugh, K. P., Eds.; Springer Singapore: Singapore, 2019; pp 581−604.
(4) Fleitas Martínez, O.; Rigueiras, P. O.; Pires, Á. d. S.; Porto, W. F.; Silva, O. N.; de la Fuente-Nunez, C.; Franco, O. L. Interference With Quorum-Sensing Signal Biosynthesis as a Promising Therapeutic Strategy Against Multidrug-Resistant Pathogens. *Front. Cell. Infect. Microbiol.* **2019**, *8*, 444.
(5) Defoirdt, T. Quorum-Sensing Systems as Targets for Antivirulence Therapy. *Trends Microbiol.* **2018**, *26*, 313−328.
(6) Feng, X.; Guo, W.; Zheng, H.; Du, J.; Luo, H.; Wu, Q.; Ren, N. Inhibition of Biofilm Formation by Chemical Uncoupler, 3, 3′, 4′, 5-Tetrachlorosalicylanilide (TCS): From the Perspective of Quorum Sensing and Biofilm Related Genes. *Biochem. Eng. J.* **2018**, *137*, 95−99.
(7) Paluch, E.; Rewak-Soroczyńska, J.; Jędrusik, I.; Mazurkiewicz, E.; Jermakow, K. Prevention of Biofilm Formation by Quorum Quenching. *Appl. Microbiol. Biotechnol.* **2020**, *104*, 1871−1881.
(8) Malešević, M.; Di Lorenzo, F.; Filipić, B.; Stanisavljević, N.; Novović, K.; Senerovic, L.; Polović, N.; Molinaro, A.; Kojić, M.; Jovčić, B. Pseudomonas Aeruginosa Quorum Sensing Inhibition by Clinical Isolate Delftia Tsuruhatensis 11304: Involvement of N-Octadecanoylhomoserine Lactones. *Sci. Rep.* **2019**, *9*, 16465.
(9) Moradali, M. F.; Ghods, S.; Rehm, B. H. A. Pseudomonas Aeruginosa Lifestyle: A Paradigm for Adaptation, Survival, and Persistence. *Front. Cell. Infect. Microbiol.* **2017**, *7*. DOI: 10.3389/fcimb.2017.00039.
(10) Ding, F.; Oinuma, K.-I.; Smalley, N. E.; Schaefer, A. L.; Hamwy, O.; Peter Greenberg, E.; Dandekar, A. A. The Pseudomonas Aeruginosa Orphan Quorum Sensing Signal Receptor QscR Regulates Global Quorum Sensing Gene Expression by Activating a Single Linked Operon. *mBio* **2018**, *9*, No. e01274.
(11) Lee, J.; Zhang, L. The Hierarchy Quorum Sensing Network in Pseudomonas Aeruginosa. *Protein Cell* **2015**, *6*, 26−41.
(12) Gebreyohannes, G.; Nyerere, A.; Bii, C.; Sbhatu, D. B. Challenges of Intervention, Treatment, and Antibiotic Resistance of Biofilm-Forming Microorganisms. *Heliyon* **2019**, *5*, No. e02192.
(13) Gram, L.; de Nys, R.; Maximilien, R.; Givskov, M.; Steinberg, P.; Kjelleberg, S. Inhibitory Effects of Secondary Metabolites from the Red Alga Delisea Pulchra on Swarming Motility of Proteus Mirabilis. *Appl. Environ. Microbiol.* **1996**, *62*, 4284−4287.
(14) Saeki, E. K.; Kobayashi, R. K. T.; Nakazato, G. Quorum Sensing System: Target to Control the Spread of Bacterial Infections. *Microb. Pathog.* **2020**, *142*, 104068.
(15) Zhou, J.-W.; Chen, T.-T.; Tan, X.-J.; Sheng, J.-Y.; Jia, A.-Q. Can the Quorum Sensing Inhibitor Resveratrol Function as an Aminoglycoside Antibiotic Accelerant against Pseudomonas Aeruginosa? *Int. J. Antimicrob. Agents* **2018**, *52*, 35−41.
(16) Kuehl, R.; Al-Bataineh, S.; Gordon, O.; Luginbuehl, R.; Otto, M.; Textor, M.; Landmann, R. Furanone at Subinhibitory Concentrations Enhances Staphylococcal Biofilm Formation by LuxS Repression. *Antimicrob. Agents Chemother.* **2009**, *53*, 4159−4166.
(17) Yang, S.; Abdel-Razek, O. A.; Cheng, F.; Bandyopadhyay, D.; Shetye, G. S.; Wang, G.; Luk, Y.-Y. Bicyclic Brominated Furanones: A New Class of Quorum Sensing Modulators That Inhibit Bacterial Biofilm Formation. *Bioorg. Med. Chem.* **2014**, *22*, 1313−1317.
(18) Hayat, S.; Muzammil, S.; Shabana; Aslam, B.; Siddique, M. H.; Saqalein, M.; Nisar, M. A. Quorum Quenching: Role of Nanoparticles as Signal Jammers in Gram-Negative Bacteria. *Future Microbiol.* **2019**, *14*, 61−72.
(19) Zhang, Y.; Nayak, T.; Hong, H.; Cai, W. Biomedical Applications of Zinc Oxide Nanomaterials. *Curr. Mol. Med.* **2013**, *13*, 1633−1645.
(20) Król, A.; Pomastowski, P.; Rafińska, K.; Railean-Plugaru, V.; Buszewski, B. Zinc Oxide Nanoparticles: Synthesis, Antiseptic Activity and Toxicity Mechanism. *Adv. Colloid Interface Sci.* **2017**, *249*, 37−52.
(21) Taccola, L.; Raffa, V.; Riggio, C.; Vittorio, O.; Iorio, M. C.; Vanacore, R.; Pietrabissa, A.; Cuschieri, A. Zinc Oxide Nanoparticles as Selective Killers of Proliferating Cells. *Int. J. Nanomed.* **2011**, *6*, 1129−1140.
(22) *GRAS Substances (SCOGS) Database, Select Committee on GRAS Substances (SCOGS) Opinion: Zinc Salts*; US Food and Drug, 2015.
(23) Siddiqi, K. S.; ur Rahman, A.; Tajuddin; Husen, A. Properties of Zinc Oxide Nanoparticles and Their Activity Against Microbes. *Nanoscale Res. Lett.* **2018**, *13*, 141.
(24) Tiwari, V.; Mishra, N.; Gadani, K.; Solanki, P. S.; Shah, N. A.; Tiwari, M. Mechanism of Anti-Bacterial Activity of Zinc Oxide Nanoparticle Against Carbapenem-Resistant Acinetobacter Baumannii. *Front. Microbiol.* **2018**, *9*, 1218.
(25) Azizi-Lalabadi, M.; Ehsani, A.; Divband, B.; Alizadeh-Sani, M. Antimicrobial Activity of Titanium Dioxide and Zinc Oxide Nanoparticles Supported in 4A Zeolite and Evaluation the Morphological Characteristic. *Sci. Rep.* **2019**, *9*, 17439.
(26) Khan, M. F.; Ansari, A. H.; Hameedullah, M.; Ahmad, E.; Husain, F. M.; Zia, Q.; Baig, U.; Zaheer, M. R.; Alam, M. M.; Khan, A. M.; AlOthman, Z. A.; Ahmad, I.; Ashraf, G. M.; Aliev, G. Sol-Gel Synthesis of Thorn-like ZnO Nanoparticles Endorsing Mechanical Stirring Effect and Their Antimicrobial Activities: Potential Role as Nano-Antibiotics. *Sci. Rep.* **2016**, *6*, 27689.
(27) Jiang, Q.; Chen, J.; Yang, C.; Yin, Y.; Yao, K. Quorum Sensing: A Prospective Therapeutic Target for Bacterial Diseases. *BioMed Res. Int.* **2019**, *2019*, 1−15.
(28) LaSarre, B.; Federle, M. J. Exploiting Quorum Sensing to Confuse Bacterial Pathogens. *MMBR, Microbiol. Mol. Biol. Rev.* **2013**, *77*, 73−111.
(29) Hentzer, M.; Givskov, M. Pharmacological Inhibition of Quorum Sensing for the Treatment of Chronic Bacterial Infections. *J. Clin. Invest.* **2003**, *112*, 1300−1307.
(30) Nafee, N.; Husari, A.; Maurer, C. K.; Lu, C.; de Rossi, C.; Steinbach, A.; Hartmann, R. W.; Lehr, C.-M.; Schneider, M. Antibiotic-Free Nanotherapeutics: Ultra-Small, Mucus-Penetrating Solid Lipid Nanoparticles Enhance the Pulmonary Delivery and Anti-Virulence Efficacy of Novel Quorum Sensing Inhibitors. *J. Contr. Release Soc.* **2014**, *192*, 131−140.
(31) Srinivasan, R.; Vigneshwari, L.; Rajavel, T.; Durgadevi, R.; Kannappan, A.; Balamurugan, K.; Pandima Devi, K.; Veera Ravi, A. Biogenic Synthesis of Silver Nanoparticles Using Piper Betle Aqueous Extract and Evaluation of Its Anti-Quorum Sensing and Antibiofilm Potential against Uropathogens with Cytotoxic Effects: An in Vitro and in Vivo Approach. *Environ. Sci. Pollut. Res.* **2018**, *25*, 10538−10554.
(32) Shah, S.; Gaikwad, S.; Nagar, S.; Kulshrestha, S.; Vaidya, V.; Nawani, N.; Pawar, S. Biofilm Inhibition and Anti-Quorum Sensing Activity of Phytosynthesized Silver Nanoparticles against the Nosocomial Pathogen Pseudomonas Aeruginosa. *Biofouling* **2019**, *35*, 34−49.
(33) Khan, R.; Khan, M.; Hameedullah, A. H.; Ansari, A.; Lohani, M. B.; Khan, R.; Ahmad, I.; Husain, F. M.; Khan, W.; Alam, M. Flower-Shaped ZnO Nanoparticles Synthesized by a Novel Approach at near-Room Temperatures with Antibacterial and Antifungal Properties. *Int. J. Nanomed.* **2014**, *9*, 853−864.
(34) Zhang, H.; Yang, D.; Ji, Y.; Ma, X.; Xu, J.; Que, D. Low Temperature Synthesis of Flowerlike ZnO Nanostructures by Cetyltrimethylammonium Bromide-Assisted Hydrothermal Process. *J. Phys. Chem. B* **2004**, *108*, 3955−3958.
(35) Lee, S.-M.; Cho, S.-N.; Cheon, J. Anisotropic Shape Control of Colloidal Inorganic Nanocrystals. *Adv. Mater.* **2003**, *15*, 441−444.
(36) Cozzoli, P. D.; Manna, L. Synthetic Strategies to Size and Shape Controlled Nanocrystals and Nanocrystal Heterostructures. In *Bio-Applications of Nanoparticles*; Chan, W. C. W., Back, N., Cohen, I. R., Lajtha, A., Lambris, J. D., Paoletti, R., Series, Eds.; Advances in Experimental Medicine and Biology; Springer New York: New York, NY, 2007; Vol. *620*, pp 1−17.

https://dx.doi.org/10.1021/acsomega.0c03634
ACS Omega 2020, 5, 32203−32215

(37) Thein, M. T.; Pung, S.-Y.; Aziz, A.; Itoh, M. Stacked ZnO Nanorods Synthesized by Solution Precipitation Method and Their Photocatalytic Activity Study. *J. Sol-Gel Sci. Technol.* **2015**, *74*, 260−271.
(38) Ebin, B.; Arıg, E.; Özkal, B.; Gürmen, S. Production and Characterization of ZnO Nanoparticles and Porous Particles by Ultrasonic Spray Pyrolysis Using a Zinc Nitrate Precursor. *Int. J. Miner., Metall. Mater.* **2012**, *19*, 651−656.
(39) Shinde, V. V.; Dalavi, D. S.; Mali, S. S.; Hong, C. K.; Kim, J. H.; Patil, P. S. Surfactant Free Microwave Assisted Synthesis of ZnO Microspheres: Study of Their Antibacterial Activity. *Appl. Surf. Sci.* **2014**, *307*, 495−502.
(40) Pourrahimi, A. M.; Liu, D.; Pallon, L. K. H.; Andersson, R. L.; Martínez Abad, A.; Lagarón, J.-M.; Hedenqvist, M. S.; Ström, V.; Gedde, U. W.; Olsson, R. T. Water-Based Synthesis and Cleaning Methods for High Purity ZnO Nanoparticles − Comparing Acetate, Chloride, Sulphate and Nitrate Zinc Salt Precursors. *RSC Adv.* **2014**, *4*, 35568−35577.
(41) Das, S.; Mukhopadhyay, S.; Chatterjee, S.; Devi, P. S.; Suresh Kumar, G. Fluorescent ZnO−Au Nanocomposite as a Probe for Elucidating Specificity in DNA Interaction. *ACS Omega* **2018**, *3*, 7494−7507.
(42) Chandrappa, K. G.; Venkatesha, T. V. Electrochemical Synthesis and Photocatalytic Property of Zinc Oxide Nanoparticles. *Nano−Micro Lett.* **2012**, *4*, 14−24.
(43) Tan, S. T.; Chen, B. J.; Sun, X. W.; Fan, W. J.; Kwok, H. S.; Zhang, X. H.; Chua, S. J. Blueshift of Optical Band Gap in ZnO Thin Films Grown by Metal-Organic Chemical-Vapor Deposition. *J. Appl. Phys.* **2005**, *98*, 013505.
(44) Amalraj, A. S.; Dharani, A. P.; Inbaraj, P. F. H.; Sivakumar, V.; Senguttuvan, G. Influence of PH on Structural, Morphological and Optical Properties of Chemically Deposited Nanocrystalline ZnO Thin Films. *J. Mater. Sci.: Mater. Electron.* **2015**, *26*, 8877−8886.
(45) Moezzi, A.; McDonagh, A. M.; Cortie, M. B. Zinc Oxide Particles: Synthesis, Properties and Applications. *Chem. Eng. J.* **2012**, *185−186*, 1−22.
(46) Morkoç, H.; Özgür, Ü. *Zinc Oxide: Fundamentals, Materials and Device Technology*; Wiley-VCH: Weinheim, 2009.
(47) Lee, K. M.; Lai, C. W.; Ngai, K. S.; Juan, J. C. Recent Developments of Zinc Oxide Based Photocatalyst in Water Treatment Technology: A Review. *Water Res.* **2016**, *88*, 428−448.
(48) Wilson, H. F.; Tang, C.; Barnard, A. S. Morphology of Zinc Oxide Nanoparticles and Nanowires: Role of Surface and Edge Energies. *J. Phys. Chem. C* **2016**, *120*, 9498−9505.
(49) Estrada-Urbina, J.; Cruz-Alonso, A.; Santander-González, M.; Méndez-Albores, A.; Vázquez-Durán, A. Nanoscale Zinc Oxide Particles for Improving the Physiological and Sanitary Quality of a Mexican Landrace of Red Maize. *Nanomaterials* **2018**, *8*, 247.
(50) Abdolmaleki, A.; Mallakpour, S.; Borandeh, S. Preparation, Characterization and Surface Morphology of Novel Optically Active Poly(Ester-Amide)/Functionalized ZnO Bionanocomposites via Ultrasonication Assisted Process. *Appl. Surf. Sci.* **2011**, *257*, 6725−6733.
(51) Noei, H.; Qiu, H.; Wang, Y.; Löffler, E.; Wöll, C.; Muhler, M. The Identification of Hydroxyl Groups on ZnO Nanoparticles by Infrared Spectroscopy. *Phys. Chem. Chem. Phys.* **2008**, *10*, 7092.
(52) *Course Notes on the Interpretation of Infrared and Raman Spectra: Mayo/Raman Spectra*; Mayo, D. W., Miller, F. A., Hannah, R. W., Eds.; John Wiley & Sons, Inc.: Hoboken, NJ, USA, 2004.
(53) Pourmbarak Mahnaie, M.; Mahmoudi, H. Effect of Glutathione-Stabilized Silver Nanoparticles on Expression of Las I and Las R of the Genes in Pseudomonas Aeruginosa Strains. *Eur. J. Med.Res.* **2020**, *25*, 17.
(54) Premanathan, M.; Karthikeyan, K.; Jeyasubramanian, K.; Manivannan, G. Selective Toxicity of ZnO Nanoparticles toward Gram-Positive Bacteria and Cancer Cells by Apoptosis through Lipid Peroxidation. *Nanomedicine* **2011**, *7*, 184−192.
(55) Saravanakkumar, D.; Sivaranjani, S.; Kaviyarasu, K.; Ayeshamariam, A.; Ravikumar, B.; Pandiarajan, S.; Veeralakshmi, C.; Jayachandran, M.; Maaza, M. Synthesis and Characterization of ZnO−CuO Nanocomposites Powder by Modified Perfume Spray Pyrolysis Method and Its Antimicrobial Investigation. *J. Semicond.* **2018**, *39*, 033001.
(56) Al-Shabib, N. A.; Husain, F. M.; Ahmed, F.; Khan, R. A.; Ahmad, I.; Alsharaeh, E.; Khan, M. S.; Hussain, A.; Rehman, M. T.; Yusuf, M.; Hassan, I.; Khan, J. M.; Ashraf, G. M.; Alsalme, A.; Al-Ajmi, M. F.; Tarasov, V. V.; Aliev, G. Biogenic Synthesis of Zinc Oxide Nanostructures from Nigella Sativa Seed: Prospective Role as Food Packaging Material Inhibiting Broad-Spectrum Quorum Sensing and Biofilm. *Sci. Rep.* **2016**, *6*, 36761.
(57) Wagh, M. S.; Patil, R. H.; Thombre, D. K.; Kulkarni, M. V.; Gade, W. N.; Kale, B. B. Evaluation of Anti-Quorum Sensing Activity of Silver Nanowires. *Appl. Microbiol. Biotechnol.* **2013**, *97*, 3593−3601.
(58) Hussain, A.; Alajmi, M. F.; Khan, M. A.; Pervez, S. A.; Ahmed, F.; Amir, S.; Husain, F. M.; Khan, M. S.; Shaik, G. M.; Hassan, I.; Khan, R. A.; Rehman, M. T. Biosynthesized Silver Nanoparticle (AgNP) From Pandanus Odorifer Leaf Extract Exhibits Anti-Metastasis and Anti-Biofilm Potentials. *Front. Microbiol.* **2019**, *10*, 8.
(59) Valderrey, A. D.; Pozuelo, M. J.; Jiménez, P. A.; Maciá, M. D.; Oliver, A.; Rotger, R. Chronic Colonization by Pseudomonas Aeruginosa of Patients with Obstructive Lung Diseases: Cystic Fibrosis, Bronchiectasis, and Chronic Obstructive Pulmonary Disease. *Diagn. Microbiol. Infect. Dis.* **2010**, *68*, 20−27.
(60) Gellatly, S. L.; Hancock, R. E. W. Pseudomonas Aeruginosa : New Insights into Pathogenesis and Host Defenses. *Pathog. Dis.* **2013**, *67*, 159−173.
(61) Sousa, A.; Pereira, M. Pseudomonas Aeruginosa Diversification during Infection Development in Cystic Fibrosis Lungs—A Review. *Pathogens* **2014**, *3*, 680−703.
(62) Ahmed, S. A. K. S.; Rudden, M.; Smyth, T. J.; Dooley, J. S. G.; Marchant, R.; Banat, I. M. Natural Quorum Sensing Inhibitors Effectively Downregulate Gene Expression of Pseudomonas Aeruginosa Virulence Factors. *Appl. Microbiol. Biotechnol.* **2019**, *103*, 3521−3535.
(63) Li, X.-H.; Lee, J.-H. Quorum Sensing-Dependent Post-Secretional Activation of Extracellular Proteases in Pseudomonas Aeruginosa. *J. Biol. Chem.* **2019**, *294*, 19635−19644.
(64) Prateeksha; Singh, B. R.; Shoeb, M.; Sharma, S.; Naqvi, A. H.; Gupta, V. K.; Singh, B. N. Scaffold of Selenium Nanovectors and Honey Phytochemicals for Inhibition of Pseudomonas Aeruginosa Quorum Sensing and Biofilm Formation. *Front. Cell. Infect. Microbiol.* **2017**, *7*, 93.
(65) Sarabhai, S.; Sharma, P.; Capalash, N. Ellagic Acid Derivatives from Terminalia Chebula Retz. Downregulate the Expression of Quorum Sensing Genes to Attenuate Pseudomonas Aeruginosa PAO1 Virulence. *PLoS One* **2013**, *8*, No. e53441.
(66) García-Lara, B.; Saucedo-Mora, M. Á.; Roldán-Sánchez, J. A.; Pérez-Eretza, B.; Ramasamy, M.; Lee, J.; Coria-Jimenez, R.; Tapia, M.; Varela-Guerrero, V.; García-Contreras, R. Inhibition of Quorum-Sensing-Dependent Virulence Factors and Biofilm Formation of Clinical and Environmental Pseudomonas Aeruginosa Strains by ZnO Nanoparticles. *Lett. Appl. Microbiol.* **2015**, *61*, 299−305.
(67) Husain, F. M.; Ahmad, I.; Khan, M. S.; Ahmad, E.; Tahseen, Q.; Khan, M. S.; Alshabib, N. A. Sub-MICs of Mentha Piperita Essential Oil and Menthol Inhibits AHL Mediated Quorum Sensing and Biofilm of Gram-Negative Bacteria. *Front. Microbiol.* **2015**, *6*, 420.
(68) Limoli, D. H.; Jones, C. J.; Wozniak, D. J. Bacterial Extracellular Polysaccharides in Biofilm Formation and Function. *Microbiol. Spectrum* **2015**, *3* (3), MB-0011-2014.
(69) Pratt, L. A.; Kolter, R. Genetic Analysis of Escherichia Coli Biofilm Formation: Roles of Flagella, Motility, Chemotaxis and Type I Pili. *Mol. Microbiol.* **1998**, *30*, 285−293.
(70) Lakshmanan, D.; Nanda, J.; Jeevaratnam, K. Inhibition of Swarming Motility of Pseudomonas Aeruginosa by Methanol Extracts of *Alpinia Officinarum* Hance. and *Cinnamomum Tamala* T. Nees and Eberm. *Nat. Prod. Res.* **2018**, *32*, 1307−1311.
(71) Sybiya Vasantha Packiavathy, I. A.; Agilandeswari, P.; Musthafa, K. S.; Karutha Pandian, S.; Veera Ravi, A. Antibiofilm and Quorum

https://dx.doi.org/10.1021/acsomega.0c03634
ACS Omega 2020, 5, 32203−32215

Sensing Inhibitory Potential of Cuminum Cyminum and Its Secondary Metabolite Methyl Eugenol against Gram Negative Bacterial Pathogens. *Food Res. Int.* **2012**, *45*, 85−92.
(72) Husain, F. M.; Ahmad, I.; Al-thubiani, A. S.; Abulreesh, H. H.; AlHazza, I. M.; Aqil, F. Leaf Extracts of Mangifera Indica L. Inhibit Quorum Sensing − Regulated Production of Virulence Factors and Biofilm in Test Bacteria. *Front. Microbiol.* **2017**, *8*, 727.
(73) Vasavi, H. S.; Arun, A. B.; Rekha, P.-D. Anti-Quorum Sensing Activity of *Psidium Guajava* L. Flavonoids against *Chromobacterium Violaceum* and Pseudomonas Aeruginosa PAO1: Quorum Sensing Inhibition by *P.* Guajava. *Microbiol. Immunol.* **2014**, *58*, 286−293.
(74) Zhou, J.-W.; Luo, H.-Z.; Jiang, H.; Jian, T.-K.; Chen, Z.-Q.; Jia, A.-Q. Hordenine: A Novel Quorum Sensing Inhibitor and Antibiofilm Agent against Pseudomonas Aeruginosa. *J. Agric. Food Chem.* **2018**, *66*, 1620−1628.
(75) Qais, F. A.; Khan, M. S.; Ahmad, I. Broad-Spectrum Quorum Sensing and Biofilm Inhibition by Green Tea against Gram-Negative Pathogenic Bacteria: Deciphering the Role of Phytocompounds through Molecular Modelling. *Microb. Pathog.* **2019**, *126*, 379−392.
(76) Wang, W.; Li, D.; Huang, X.; Yang, H.; Qiu, Z.; Zou, L.; Liang, Q.; Shi, Y.; Wu, Y.; Wu, S.; Yang, C.; Li, Y. Study on Antibacterial and Quorum-Sensing Inhibition Activities of Cinnamomum Camphora Leaf Essential Oil. *Molecules* **2019**, *24* (20), 3792.
(77) Al-Shabib, N. A.; Husain, F. M.; Ahmad, N.; Qais, F. A.; Khan, A.; Khan, A.; Khan, M. S.; Khan, J. M.; Shahzad, S. A.; Ahmad, I. Facile Synthesis of Tin Oxide Hollow Nanoflowers Interfering with Quorum Sensing-Regulated Functions and Bacterial Biofilms. *J. Nanomater.* **2018**, *2018*, 1−11.
(78) Hasan, I.; Qais, F. A.; Husain, F. M.; Khan, R. A.; Alsalme, A.; Alenazi, B.; Usman, M.; Jaafar, M. H.; Ahmad, I. Eco-Friendly Green Synthesis of Dextrin Based Poly (Methyl Methacrylate) Grafted Silver Nanocomposites and Their Antibacterial and Antibiofilm Efficacy against Multi-Drug Resistance Pathogens. *J. Cleaner Prod.* **2019**, *230*, 1148−1155.
(79) Khan, F.; Manivasagan, P.; Lee, J.-W.; Pham, D.; Oh, J.; Kim, Y.-M. Fucoidan-Stabilized Gold Nanoparticle-Mediated Biofilm Inhibition, Attenuation of Virulence and Motility Properties in Pseudomonas Aeruginosa PAO1. *Mar. Drugs* **2019**, *17*, 208.
(80) Pearson, J. P.; Gray, K. M.; Passador, L.; Tucker, K. D.; Eberhard, A.; Iglewski, B. H.; Greenberg, E. P. Structure of the Autoinducer Required for Expression of Pseudomonas Aeruginosa Virulence Genes. *Proc. Natl. Acad. Sci. U.S.A.* **1994**, *91*, 197−201.
(81) Pesci, E. C.; Milbank, J. B. J.; Pearson, J. P.; McKnight, S.; Kende, A. S.; Greenberg, E. P.; Iglewski, B. H. Quinolone Signaling in the Cell-to-Cell Communication System of Pseudomonas Aeruginosa. *Proc. Natl. Acad. Sci. U.S.A.* **1999**, *96*, 11229−11234.
(82) McKnight, S. L.; Iglewski, B. H.; Pesci, E. C. The Pseudomonas Quinolone Signal Regulates Rhl Quorum Sensing in Pseudomonas Aeruginosa. *J. Bacteriol.* **2000**, *182*, 2702−2708.
(83) Diggle, S. P.; Winzer, K.; Chhabra, S. R.; Worrall, K. E.; Cámara, M.; Williams, P. The Pseudomonas Aeruginosa Quinolone Signal Molecule Overcomes the Cell Density-Dependency of the Quorum Sensing Hierarchy, Regulates Rhl-Dependent Genes at the Onset of Stationary Phase and Can Be Produced in the Absence of LasR: PQS Regulation of Rhl-Dependent Phenotypes. *Mol. Microbiol.* **2003**, *50*, 29−43.
(84) Husain, F. M.; Ahmad, I.; Baig, M. H.; Khan, M. S.; Khan, M. S.; Hassan, I.; Al-Shabib, N. A. Broad-Spectrum Inhibition of AHL-Regulated Virulence Factors and Biofilms by Sub-Inhibitory Concentrations of Ceftazidime. *RSC Adv.* **2016**, *6*, 27952−27962.
(85) Boles, B. R.; Horswill, A. R. Agr-Mediated Dispersal of Staphylococcus Aureus Biofilms. *PLoS Pathog.* **2008**, *4*, No. e1000052.
(86) Sandasi, M.; Leonard, C. M.; Van Vuuren, S. F.; Viljoen, A. M. Peppermint (Mentha Piperita) Inhibits Microbial Biofilms in Vitro. *S. Afr. J. Bot.* **2011**, *77*, 80−85.
(87) Saxena, P.; Joshi, Y.; Rawat, K.; Bisht, R. Biofilms: Architecture, Resistance, Quorum Sensing and Control Mechanisms. *Indian J. Microbiol.* **2019**, *59*, 3−12.
(88) Sharma, D.; Misba, L.; Khan, A. U. Antibiotics versus Biofilm: An Emerging Battleground in Microbial Communities. *Antimicrob. Resist. Infect. Contr.* **2019**, *8*, 76.
(89) Saini, H.; Chhibber, S.; Harjai, K. Azithromycin and Ciprofloxacin: A Possible Synergistic Combination against Pseudomonas Aeruginosa Biofilm-Associated Urinary Tract Infections. *Int. J. Antimicrob. Agents* **2015**, *45*, 359−367.
(90) Al-Shabib, N. A.; Husain, F. M.; Hassan, I.; Khan, M. S.; Ahmed, F.; Qais, F. A.; Oves, M.; Rahman, M.; Khan, R. A.; Khan, A.; Hussain, A.; Alhazza, I. M.; Aman, S.; Noor, S.; Ebaid, H.; Al-Tamimi, J.; Khan, J. M.; Al-Ghadeer, A. R. M.; Khan, M. K. A.; Ahmad, I. Biofabrication of Zinc Oxide Nanoparticle from *Ochradenus Baccatus* Leaves: Broad-Spectrum Antibiofilm Activity, Protein Binding Studies, and *In Vivo* Toxicity and Stress Studies. *J. Nanomater.* **2018**, *2018*, 1−14.
(91) Al-Shabib, N. A.; Husain, F. M.; Ahmed, F.; Khan, R. A.; Khan, M. S.; Ansari, F. A.; Alam, M. Z.; Ahmed, M. A.; Khan, M. S.; Baig, M. H.; Khan, J. M.; Shahzad, S. A.; Arshad, M.; Alyousef, A.; Ahmad, I. Low Temperature Synthesis of Superparamagnetic Iron Oxide (Fe3O4) Nanoparticles and Their ROS Mediated Inhibition of Biofilm Formed by Food-Associated Bacteria. *Front. Microbiol.* **2018**, *9*, 2567.
(92) Parasuraman, P.; Antony, A. P.; B, S. L. S.; Sharan, A.; Siddhardha, B.; Kasinathan, K.; Bahkali, N. A.; Dawoud, T. M. S.; Syed, A. Antimicrobial Photodynamic Activity of Toluidine Blue Encapsulated in Mesoporous Silica Nanoparticles against Pseudomonas Aeruginosa and Staphylococcus Aureus. *Biofouling* **2019**, *35*, 89−103.
(93) Husain, F. M.; Ahmad, I. Doxycycline Interferes with Quorum Sensing-Mediated Virulence Factors and Biofilm Formation in Gram-Negative Bacteria. *World J. Microbiol. Biotechnol.* **2013**, *29*, 949−957.
(94) Musthafa, K. S.; Sivamaruthi, B. S.; Pandian, S. K.; Ravi, A. V. Quorum Sensing Inhibition in Pseudomonas Aeruginosa PAO1 by Antagonistic Compound Phenylacetic Acid. *Curr. Microbiol.* **2012**, *65*, 475−480.
(95) Blosser, R. S.; Gray, K. M. Extraction of Violacein from Chromobacterium Violaceum Provides a New Quantitative Bioassay for N-Acyl Homoserine Lactone Autoinducers. *J. Microbiol. Methods* **2000**, *40*, 47−55.
(96) Adonizio, A.; Kong, K.-F.; Mathee, K. Inhibition of Quorum Sensing-Controlled Virulence Factor Production in Pseudomonas Aeruginosa by South Florida Plant Extracts. *Antimicrob. Agents Chemother.* **2008**, *52*, 198−203.
(97) Kessler, E.; Safrin, M.; Olson, J. C.; Ohman, D. E. Secreted LasA of Pseudomonas Aeruginosa Is a Staphylolytic Protease. *J. Biol. Chem.* **1993**, *268*, 7503−7508.
(98) Essar, D. W.; Eberly, L.; Hadero, A.; Crawford, I. P. Identification and Characterization of Genes for a Second Anthranilate Synthase in Pseudomonas Aeruginosa: Interchangeability of the Two Anthranilate Synthases and Evolutionary Implications. *J. Bacteriol.* **1990**, *172*, 884−900.
(99) Huston, A. L.; Methe, B.; Deming, J. W. Purification, Characterization, and Sequencing of an Extracellular Cold-Active Aminopeptidase Produced by Marine Psychrophile Colwellia Psychrerythraea Strain 34H. *Appl. Environ. Microbiol.* **2004**, *70*, 3321−3328.
(100) Dubois, M.; Gilles, K.; Hamilton, J. K.; Rebers, P. A.; Smith, F. A Colorimetric Method for the Determination of Sugars. *Nature* **1951**, *168*, 167.
(101) Cugini, C.; Calfee, M. W.; Farrow, J. M.; Morales, D. K.; Pesci, E. C.; Hogan, D. A. Farnesol, a Common Sesquiterpene, Inhibits PQS Production in Pseudomonas Aeruginosa. *Mol. Microbiol.* **2007**, *65*, 896−906.
(102) Sandasi, M.; Leonard, C. M.; Viljoen, A. M. The in Vitro Antibiofilm Activity of Selected Culinary Herbs and Medicinal Plants against Listeria Monocytogenes: Anti-Biofilm Activity. *Lett. Appl. Microbiol.* **2010**, *50*, 30−35.
(103) O'Toole, G. A.; Kolter, R. Initiation of Biofilm Formation in Pseudomonas Fluorescens WCS365 Proceeds via Multiple, Con-

https://dx.doi.org/10.1021/acsomega.0c03634
ACS Omega 2020, 5, 32203−32215

vergent Signalling Pathways: A Genetic Analysis. *Mol. Microbiol.* **1998**, *28*, 449−461.

https://dx.doi.org/10.1021/acsomega.0c03634
ACS Omega 2020, 5, 32203−32215